Comparison of Native and Mutant Proteins Provides a Sequence-Specific Assignment of the Cysteinyl Ligand Proton NMR Resonances in the 2[Fe_4S_4] Ferredoxin from *Clostridium pasteurianum*†

Sergio D. B. Scrofani,‡,§ Phillip S. Brereton,§ Amanda M. Hamer,§ Megan J. Lavery,§ Sharon G. McDowall,‡ Graham A. Vincent,‡ Robert T. C. Brownlee,*,‡ Nicholas J. Hoogenraad,‡ Maruse Sadek,‡ and Anthony G. Wedd*,§

Departments of Chemistry and Biochemistry and the Centre for Protein and Enzyme Technology, La Trobe University, Bundoora, Victoria 3083, Australia, and School of Chemistry, University of Melbourne, Parkville, Victoria 3052, Australia

Received July 14, 1994; Revised Manuscript Received August 30, 1994⊗

ABSTRACT: A sequence-specific assignment is presented for the eight low-field paramagnetically shifted cysteinyl ligand proton NMR resonances in the 2[Fe_4S_4] ferredoxin from *Clostridium pasteurianum*. The assignment is based upon comparison of chemical shifts in 1D and 2D NMR spectra of native oxidized protein and those of three mutants. The mutant proteins G12A and G41A were designed to produce minor local structural changes (hence small chemical shift perturbations) in either cluster I (glycine 12 to alanine) or in cluster II (glycine 41 to alanine). Observed chemical shift changes in spectra of the double mutant G12,41A support the interpretation. The comparison is aided by structural models derived from the crystal structure of the related ferredoxin from *Peptococcus aerogenes*. Each of the eight low-field resonances is assigned to a β-proton from a different cysteinyl ligand, and so connectivities established from previous TOCSY and HMQC data allow assignment of all 24 cysteinyl ligand protons.

The ferredoxin from *Clostridium pasteurianum* (*Cp*Fd:[1] two $[Fe_4S_4]^{2+}$; 6203 Da) was the first iron−sulfur protein discovered (Mortenson et al., 1962) and acts as an electronic shuttle between catabolic and anabolic pathways, servicing a number of enzyme systems including nitrogenase and hydrogenase (Thauer & Schonheit, 1982; Cammack, 1992). Its primary structure (Figure 1) has 70% homology with that from *Peptococcus aerogenes* (*Pa*Fd), whose crystal structure is available (Adman et al., 1973; Backes et al., 1991).

Molecular control of electron transfer in redox proteins is of intense current interest as the polypeptide structure surrounding the redox center apparently fine tunes both the potential and the rate of electron transfer [see, for example, Palmer (1991) and Langen et al. (1992)]. NMR provides detailed structural information for diamagnetic proteins, but its application to paramagnetic proteins such as *Cp*Fd[2] is complicated by the shifting and broadening of resonances (Bertini & Luchinat, 1986; Busse et al., 1991; Bertini et al., 1992; Sadek et al., 1993). Such properties have not prevented partial structural characterization of some iron−sulfur proteins by NMR [see, for example, Oh and Markley (1990a−c), Gaillard et al. (1992), Cheng et al. (1992), and Chae et al. (1994)], and a complete sequence-specific assignment of shifted cysteinyl ligand ^1H resonances has been achieved for certain HiPIP proteins which contain a single Fe_4S_4 center (Banci et al., 1993).

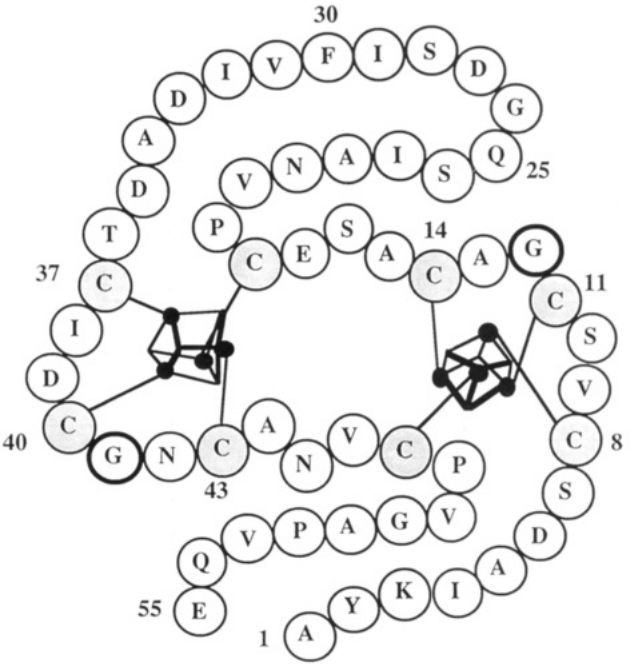

FIGURE 1: Simple two-dimensional representation of *Cp*Fd. The cysteinyl ligands are shaded, and the points of mutation, Gly 12 and Gly 41, are outlined.

† This research was supported by grants to R.T.C.B. and A.G.W. from the Australian Research Council.

* To whom correspondence should be addressed.

‡ La Trobe University.

§ University of Melbourne.

⊗ Abstract published in *Advance ACS Abstracts,* October 15, 1994.

[1] Abbreviations: *Cau*Fd, ferredoxin from *Clostridium acidi urici*; *Cp*Fd, ferredoxin from *Clostridium pasteurianum*; EXSY, exchange spectroscopy; DSS, sodium 2,2-dimethyl-2-silapentane-5-sulfonate; G12A, glycine 12 to alanine mutant *Cp*Fd; G41A, glycine 41 to alanine mutant *Cp*Fd; G12,41A, glycine 12 to alanine and glycine 41 to alanine double mutant *Cp*Fd; GARP, globally optimized alternating phase rectangular pulse; HMQC, heteronuclear multiple quantum coherence; HiPIP, high-potential iron protein; IPTG, isopropyl-β-D-thiogalactopyranoside; NOE, nuclear Overhauser effect; NOESY, nuclear Overhauser enhanced spectroscopy; *Pa*Fd, ferredoxin from *Peptococcus aerogenes*; P19K, proline 19 to lysine mutant *Cp*Fd; P48K, proline 48 to lysine mutant *Cp*Fd; TOCSY, total correlated spectroscopy; TPPI, time-proportional phase incrementation; X-gal, 5-bromo-4-chloro-3-indolyl-β-D-galactoside.

[2] While the ground state of an $[Fe_4S_4(S\text{-}cys)_4]^{2-}$ cluster is S = 0, paramagnetism at normal temperatures arises from population of excited states: $\mu_{eff} \sim 2\ \mu_B$ per cluster (Gaillard et al., 1987).

0006-2960/94/0433-14486$04.50/0

*Cp*Fd and related proteins are a particular challenge as two [Fe_4S_4] centers are present, whose nearest atoms are separated by approximately 9 Å. However, steady progress led to identification of the 16 H^{β} and seven of the eight H^{α} ^1H resonances of the eight cluster cysteinyl ligands of *Cp*Fd plus assignment of the resonances to clusters I or II (Figure 1) (Packer et al., 1977; Bertini et al., 1990, 1991, 1992; Busse et al., 1991; Sadek et al., 1993). This progress culminated recently in a sequence-specific assignment of the cysteinyl protons in the closely related ferredoxin from *Clostridium acidi urici* (*Cau*Fd), which was derived from COSY, TOCSY, NOESY and, crucially, EXSY spectra of the oxidized and one- and two-electron reduced forms (Bertini et al., 1994). In addition, the eight C^{β} and six of the eight C^{α} ^{13}C resonances were observed by HMQC experiments. These data on the hyperfine-shifted resonances indicate that delocalization of electron spin from the cluster to the H^{α}, H^{β}, and C^{α} atoms is mediated by the p_{π} orbitals of the cysteinyl sulfurs. This assignment was extended logically to *Cp*Fd.

Recombinant and mutant forms of *Cp*Fd have been isolated recently (Bauer et al., 1990; Smith et al., 1991; Davasse & Moulis, 1992), and some mutant forms have been examined by ^1H NMR (Gaillard et al., 1993b). The hyperfine-shifted resonances are very sensitive to structure, i.e., to amino acid substitution. Our approach has been to design mutant forms with minor local structural changes to minimize chemical shift perturbations. To this end, advantage has been taken of the pseudo 2-fold symmetry of this protein (Figures 1 and 2) to design and produce mutants G12A and G41A in which an alanine residue is substituted for the native glycine which forms part of the CysXXCys-GlyXCys sequence fragments characteristic of 8Fe ferredoxins. These fragments provide three of the four cysteinyl ligands to each cluster. The double mutant G12,41A has also been expressed to confirm that these mutations produce local structural effects only.

This independent approach achieves a self-consistent sequence-specific assignment of the cysteinyl ligand ^1H resonances of *Cp*Fd and confirms a recently published assignment based on data for the related ferredoxin *Cau*Fd (Bertini et al., 1994). An evaluation of stereospecific assignments of the cysteinyl ligand resonances is included.

MATERIALS AND METHODS

The enzymes *Pst*1 and *Taq* polymerase were obtained from Promega. *Kpn*1 and T_4 polynucleotide kinase were purchased from NE Biolabs. *Sma*1 was obtained from BRL. Calf intestine alkaline phosphatase and the Klenow fragment were from Boehringer Mannheim. IPTG, X-gal, ampicillin, chloramphenicol, kanamycin, agarose, DNase-free pancreatic RNase, deoxyribonuclease 1, PMSF, horse heart cytochrome *c*, spinach ferredoxin-$NADP^+$ oxidoreductase, and NADPH were all from Sigma. The Sequenase kit was from USB, and the Mutagene kit was from Bio-Rad. Bacterial growth media were from Oxoid. The chromatographic column materials used were DE-52 (Whatman), Sephadex G-75 (Pharmacia), Qiagen-5 (Qiagen), and C-18 Sep-Pak (Waters Associates). The radionucleotides, [α-^{35}S]dATP and [γ-^{32}P]-ATP were purchased from Bresatec.

DNA manipulations [plasmid preparations (alkaline lysis), ligations and transformations] were as described in Sambrook et al. (1989).

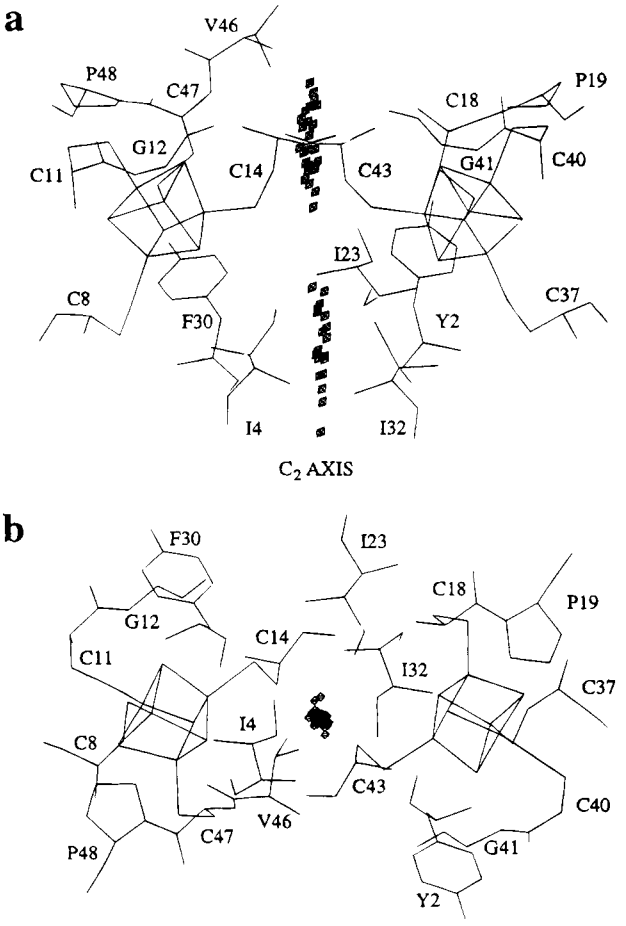

FIGURE 2: (a) *Cp*Fd structural model in the region of the clusters. The boxes represent the center points of lines which connect symmetry-related atoms (see text). (b) The same model rotated by 90°, showing that the center points indeed form a line. The symmetry relationship as shown is observed in the X-ray structure of *Pa*Fd and all calculated models of *Cp*Fd.

Genomic DNA Preparation. *Cp* cells were grown in glucose media (Rabinowitz, 1972) to mid-log phase. Isolated chromosomal DNA was dissolved in TE buffer to a final concentration of about 0.4 $\mu g\ \mu L^{-1}$, and the size of the DNA was verified to be greater than 12 000 bp.

Oligonucleotides. Two oligonucleotides were designed using the reported gene sequence of the *Cp*Fd gene (Graves et al., 1985) and synthesized on an Applied Biosystems DNA synthesizer Model 380A. A 22-mer (5′-CCCCCTAATATTTTCTTCAATT-3′) was complementary to the nontranscribed strand between base pairs 426−447. A 24-mer (5′-ATAAGTTATGGTAAACTTATGATT-3′) was complementary to the transcribed strand between base pairs 120−143. Purity was assessed by electrophoresis on a 20% urea−polyacrylamide gel. Samples that contained significant amounts of failure sequences were purified on this gel, the required band was excized, and the DNA fragment was recovered by chromatography on a C-18 Sep-Pak reverse-phase column.

Cloning and DNA Sequencing. A *Cp*Fd gene fragment was isolated via the polymerase chain reaction (Saiki et al., 1987) using *Cp* chromosomal DNA isolated as a template (Graves et al., 1985). A band of the expected size (328 bp) was visualized with ethidium bromide on a 2% agarose−TBE gel and was the sole product of the PCR. The PCR fragment was 5′-phosphorylated, and the Klenow fragment

was used to fill in any recessed 3′ ends. This blunt-ended fragment was ligated into the dephosphorylated *Sma*1 site of the plasmid pTZ19U (Mutagene). The construct was used to transform *Escherichia coli* MV1190. The fragment was then subcloned into the *Kpn*1 and *Pst*1 sites of pTZ18U. Ampicillin-resistant colonies, which had lost the ability to produce a functional β-galactoside and therefore appeared white on X-gal/IPTG plates, were selected. Sanger dideoxy sequencing on single-stranded plasmid, isolated either by Qiagen columns or phenol/chloroform extractions, was achieved using a Sequenase kit with [α-^{35}S]dATP. Autoradiography performed at −70 °C for around 20 h confirmed that the cloned fragment was identical to that reported previously for *Cp*Fd (Graves et al., 1985) except for position 351 where a G for A substitution had occurred in the nontranscribed strand.

Mutagenesis. Site-directed mutagenesis employed a Mutagene kit (Kunkel, 1985). The plasmids pTZ18U/*Cp*Fd and pTZ19U/*Cp*Fd were transformed into *E. coli* CJ236. Single-stranded DNA isolated from *E. coli* CJ236 containing pTZ18U/*Cp*Fd was used as the template for DNA synthesis for the production of the G12A mutant. The sequence of the primer used to produce the G12A mutant was 5′-GTAAGCTGTG^{C}/$_{T}$CGCTTGTGCT-3′. After mutagenesis and sequencing, the G12A mutant was subcloned into the *Kpn*1 and *Pst*1 sites of pTZ19U for protein expression. For the G41A mutant, single-stranded DNA was isolated from *E. coli* CJ236 containing the pTZ19U/*Cp*Fd plasmid and used as a template for DNA synthesis. The sequence of the primer used to produce the G41A mutant was 5′-AGCACAGTTA^{G}/$_{A}$CACAGTCGAT-3′. The double mutant G12,41A was produced using single-stranded DNA isolated from *E. coli* CJ236 containing pTZ19U/G12A*Cp*Fd. The second mutation was introduced using the same primer used for G41A production.

Protein Expression. The recombinant and three mutant forms of *Cp*Fd were expressed in a T7 polymerase promoter system. The plasmids were transformed into *E. coli* BL21DE3[pLysS] (Studier, 1991). Overnight cultures were grown in LB medium containing ampicillin (100 μg mL^{-1}) and chloramphenicol (33 μg mL^{-1}). The following day 1-L cultures were inoculated with 2 mL of the overnight culture. The cells were grown until OD_{600} = 1.0−1.5 and induced with IPTG (0.4 mM), after which ammonium ferrous sulfate (50 μM) was added. The cells were pelleted by centrifugation for 15 min (7000*g* at 4 °C) and resuspended (3 mL g^{-1}) in *E. coli* lysis buffer (Sambrook et al., 1989) containing PMSF (133 μM) and Triton X-100 (0.1%). The cells were lyzed by a freeze−thaw cycle, deoxyribonuclease 1 (10 μg mL^{-1}) was added, and the mixture was incubated at 37 °C until it was no longer viscous (around 1 h). After centrifugation for 25 min (23000*g* at 4 °C), the supernatant was decanted, added to an equal volume of 50 mM Tris-HCl, pH 7.4, and applied to a DE-52 column. Ferredoxin was eluted with a 0.07−0.27 M NaCl gradient in 0.15 M Tris-HCl, pH 7.4. Fractions with A_{390}/A_{280} > 0.25 were combined and treated with ammonium sulfate to 60% saturation. After the precipitate was discarded, the ammonium sulfate concentration was increased to 100% saturation, precipitating *Cp*Fd. After dissolution in 50 mM potassium phosphate, pH 7.2, and gel filtration on a Sephadex G-75 column, fractions with A_{390}/A_{280} > 0.80 were combined and concentrated using an Amicon ultrafiltration cell equipped with a YM3 membrane. Yields were around 1, 0.7, and 0.5 mg L^{-1} of starting culture for the recombinant, single, and double mutant proteins, respectively.

Protein Sequencing. The first 15 amino acids of the recombinant and G12A proteins were confirmed by sequential Edman degradation.

Metal Stoichiometry. Metal analysis was carried out using a Plasmaquad inductively coupled plasma mass spectrometer (VG Elemental). Native and recombinant *Cp*Fd and the G12A mutant were analyzed for metal content (200 μg of protein/10 mL). The following metals were assayed: ^{52}Cr, ^{55}Mn, ^{57}Fe, ^{58}Ni, ^{59}Co, ^{63}Cu, ^{64}Zn, and ^{111}Cd. Iron was the only metal found in significant quantity. Protein concentrations were measured by UV−vis spectrophotometry using an extinction coefficient of 30 600 M^{-1} cm^{-1} at 390 nm (Rabinowitz, 1972; Moulis & Meyer, 1982). This value was confirmed by quantitative drying of a *Cp*Fd sample of known absorbance suspended in ammonium carbonate buffer.

Electrochemistry. Square wave voltammetry was carried out at a pyrolytic graphite electrode at 25 °C using a Cypress CS-1087 instrument (Armstrong et al., 1984). In all cases, *Cp*Fd samples (200 μm) were dissolved in 20 mM Tris-HCl, pH 7.5, containing 0.1 M NaCl and were examined in the presence of 2.8 mM $[Cr(en)_3]Cl_3$. A Cr:*Cp*Fd ratio of 14:1 provides optimum current response.

Activity Assays. Ferredoxin activity was assayed for by the reduction of horse heart cytochrome *c* (Zanetti & Curti, 1980). Assays were carried out in solutions containing 50 mM Tris-HCl (pH 7.5) and 1 mg mL^{-1} bovine serum albumin at 25 °C. Spinach ferredoxin-NADP^{+} reductase (31 nM) was used to catalyze the reduction of ferredoxin by NADPH (0.3 mM). The subsequent reduction of cytochrome *c* (50 μM) by ferredoxin (0.4 μM) was followed at 550 nm assuming an extinction coefficient of 20 000 M^{-1} cm^{-1} (Coghlan & Vickery, 1991). Specific activity is defined as micromole of cytochrome *c* reduced minute^{-1} (milligram of ferredoxin)$^{-1}$.

Molecular Modeling. All molecular modeling and minimization methods were performed using both the Insight II and Discover computer software packages from BIOSYM. The computer molecular model of *Cp*Fd was derived by the homology approach (Blundell et al., 1983, 1988) from the known X-ray structure of *Pa*Fd[3] (Adman et al., 1973; Backes et al., 1991). This method requires force-field parameters for all atom types within the molecule of interest including the iron atoms. However, reliable iron parameters were not available, although progress in modeling iron−sulfur systems has been made recently (Banci et al., 1992). We chose to test the parameters adapted from the force field contained within the Insight/Discover packages and optimize the energy minimization procedure on the X-ray structure of *Pa*Fd before applying the method to the optimization of *Cp*Fd structural models. The Fe−S bonds were restrained. A cutoff set to 11 Å was applied to the van der Waals and electrostatic terms, and a distance-dependent dielectric constant was used. No water molecules were incorporated in the analysis.

[3] In order to correlate the primary sequences, numbering after residue 23 in *Pa*Fd is decreased by one compared to *Cp*Fd. Consequently, cysteinyl residues 37, 40, 43, and 47 in *Cp*Fd correspond to residues 36, 39, 42, and 46, respectively, in *Pa*Fd (Backes et al., 1991).

Optimization of *Pa*Fd increased the separation of the clusters: the closest approach, Fe 67(Cys 42)−Fe 58 (Cys 14),[4] increased from 8.8 to 9.5 Å. Changes in torsional angles $H^{\beta}-C^{\beta}-S^{\gamma}-Fe$ (between 10 and 30°) within the residues Cys 11, 39, and 42 were the only other significant changes involving cysteinyl residues. The overall shape of the molecule was conserved with the rms = 0.69 Å/atom for overlaying the backbones of the X-ray structure and the optimized model of *Pa*Fd. The same force field applied to the X-ray structure of *Pa*Fd, but with the primary sequence changed to match that of *Cp*Fd, produced a model with similar separation of the clusters [Fe 67(Cys 43)−Fe 58-(Cys 14), 9.6 Å].

NMR Experiments. All NMR spectra were recorded on oxidized *Cp*Fd dissolved in D_2O (pH 7.2, 5 mM). Proton chemical shifts were referenced to the H_2O signal at 4.78 ppm (298 K). Carbon chemical shifts were referenced to external DSS in H_2O. Unless otherwise specified, all spectra were recorded at 298 K.

1D ^1H spectra were recorded at 400.13 MHz on a Bruker AM-400/WB spectrometer equipped with an Aspect 3000 computer. A spectral width of 11 905 Hz was used to include the hyperfine-shifted resonances (8−18 ppm). The FID was collected with 8192 real data points resulting in a digital resolution of 0.004 ppm. However, the estimated chemical shift accuracy of broad resonances was ±0.02 ppm.

The following 2D spectra were recorded at 400.13 MHz: 10−100 ms NOESY (Macura & Ernst, 1980); 10−80 ms TOCSY (Bax & Davis, 1985); coupled and GARP (Shaka et al., 1985) decoupled {$^1H-^{13}C$}HMQC (Bax et al., 1983), which were recorded at natural abundance. All 2D spectra were acquired in the phase-sensitive mode, with sequential acquisition in the ω_2 dimension. Filter widths, dead times, and receiver phases were manipulated to minimize phase corrections in ω_2. For homonuclear experiments, spectral widths of 4950 or 11 905 Hz were generally utilized in both dimensions. The shorter spectral width was employed to increase digital resolution in the diamagnetic spectral region. Generally, 4096 Bruker complex data points were acquired in ω_2, except for fast-recycle time experiments where 2048 data points were collected. All 2D experiments were recorded with 384−768 increments in ω_1. Quadrature detection was achieved in the ω_2 dimension by TPPI (Marion & Wüthrich, 1983). Low power irradiation of residual water was normally required. For NOESY spectra, a 180° composite pulse placed in the middle of the mixing time was employed to prevent further relaxation recovery of the residual water peak (Freeman et al., 1988). Zero quantum coherences were not suppressed. TOCSY spectra were acquired in reverse mode using the MLEV-17 mixing scheme, flanked by 500-μs trim pulses (Bax & Davis, 1985). For the HMQC experiments ^1H and ^{13}C spectral widths were 11 905 and 23 810 Hz, respectively. A coupling evolution period of 1.9 ms was used to optimize the coherence transfer, which depends on both the size of CH coupling and the fast relaxation of cysteinyl protons.

Two experiments were recorded on a Bruker AMX-500 spectrometer: Fast NOESY (10 ms mixing time) and ^{13}C GARP decoupled {$^1H-^{13}C$}HMQC spectra, both in the phase-sensitive mode with simultaneous acquisition in ω_2 (States et al., 1982). A spectral width of 20 000 Hz was utilized in both dimensions for the NOESY spectrum, where 1024 complex data pairs in ω_2 and 3584 transients for each of the 264 increments in ω_1 were collected. The total recycle time was 51 ms, of which 25 ms was used for low power irradiation of residual water. For the HMQC spectrum, the ^1H and ^{13}C spectral widths used were 15 151 and 20 123 Hz, respectively. 4096 complex data points were acquired in ω_2 with 408 increments in ω_1. 256 transients were collected per t_1 increment with a total recycle time of 672 ms, which incorporated low power irradiation of residual water of 500 ms. An evolution period of 3.52 ms was used.

All data were processed on a Sun SPARCstation-2 using FELIX software (version 1.1) from Hare Research Inc. Spectral windows were optimized iteratively for each 2D spectrum but 60−80° shifted square sine bells were generally used in both dimensions, zero filled to form 2K × 2K real matrices. For the observation of broad peaks, the square sine window functions were applied only over the first 300 data points in both dimensions and zero filled to a 1K × 1K real matrix. When required, data were phased corrected, and a polynomial baseline correction was applied to ω_2 before the second Fourier transform.

RESULTS AND DISCUSSION

Application of the classic NMR methods used to generate three-dimensional molecular structures is restricted in paramagnetic proteins as relaxation effects can prevent the observation of crucial NOE cross-peaks (Sette et al., 1993). In such circumstances, interpretation of solution NMR data is assisted greatly by X-ray crystallographic information. The latter does not exist for *Cp*Fd but does for *Pa*Fd, which has 70% homology (Adman et al., 1973; Backes et al., 1991).

Structural Model of CpFd. We have generated optimized *Pa*Fd and *Cp*Fd structural models from the *Pa*Fd structure to assist: (i) detailed exploration of the pseudo-symmetry of *Cp*Fd; (ii) design of appropriate mutant forms; (iii) assignment of NMR data. Comparison of the X-ray structure of *Pa*Fd with the optimized *Pa*Fd and *Cp*Fd models permits possible artifacts of optimization to be distinguished from genuine structural differences. Different relative orientations of Cys 14 and Cys 43 side chains are predicted, a direct consequence of variation in the peptide segment 14−18 which connects the clusters (Figure 1). In particular, significant stereochemical and polarity changes occur at residues 15 and 16: Lys-Pro in *Pa*Fd to Ala-Ser in *Cp*Fd. New hydrogen bonds (Ser 16 $H^{\gamma}\cdots$Gly 12 CO, Ser 16 NH$\cdots$Ala 13 CO, and Asn 42 $H^{\delta}\cdots$Glu 17 CO) are predicted to lead to a change in the position of Cys 14 and also of the aromatic ring of Phe 30 in *Cp*Fd as compared to Tyr 29 in *Pa*Fd.

The other significant structural change between the optimized *Pa*Fd and *Cp*Fd models is in the positioning of residues Cys 8, 36 (37). In the *Cp*Fd model, protons within these residues are up to 0.9 Å more distant from the center of the cluster to which the specific residue is not coordinated. Again, the regions next to these cysteinyl residues are not conserved, and the replacements involve residues with different steric and electronic properties (Cys 8-Ile 9-Ala 10 to Cys 8-Val 9-Ser 10 and Asp 34-Ser 35-Cys 36 to Asp 35-Thr 36-Cys 37).

Several structural aspects of *Cp*Fd predicted by the structural model are confirmed experimentally. For example,

[4] The numbering of iron and sulfur atoms in Fe_4S_4 clusters is taken from *Pa*Fd crystal structure coordinates (Backes et al., 1991).

short sections of anti-parallel β-sheet structure in *Cp*Fd are identified by NOE interactions in the (2−5; 51−55) and (24−26; 29−31) regions (S. D. B. Scrofani, R. T. C. Brownlee, M. Sadek, and A. G. Wedd, manuscript in preparation). Such findings reinforce confidence that the structural model reproduces the essential features of the structure of *Cp*Fd, but predictions can only be confirmed by experiment.

Pseudo-Symmetry in the CpFd Structural Model. A detailed examination of the *Pa*Fd X-ray structure (Backes et al., 1991) and the *Cp*Fd structural model confirms the presence of a remarkable 2-fold axis of pseudo-symmetry based upon clusters I and II and the pairs of sequence CysXXCysGlyXCysAla (*Cp*Fd: 8−15; 37−44) and CysPro-Val (47−49; 18−20). The atoms of each of the defined residues, the aromatic rings of Phe 30 and Tyr 2, the side chains of Ile 4 and Ile 32, and the δ-methyl groups of Val 46 and Ile 23 are interchanged by the C_2 axis illustrated in Figure 2. This leads to similar patterns of hydrogen bonds around each cluster and similar dihedral angles associated with pairs of cysteinyl ligands (Backes et al., 1991). In particular, the cysteinyl ligands from clusters I and II fall into symmetry-related pairs (8, 37), (11, 40), (14, 43), and (47, 18).

As is apparent in Figure 2, the clusters face each other with Fe_2S_2 planes to which ligands Cys 14, 47 (cluster I) and Cys 43, 18 (cluster II) are bound.[5] The intervening space between the clusters is occupied by the side chains of Cys 14 and Cys 43 and four methyl groups supplied by residues Ile 4, Ile 32, Val 46, and Ile 23. The latter arrange in pairs on either side of a plane defined by the C^β and S^γ atoms of these cysteinyl residues.

The structural model indicates that no gross alteration in tertiary structure is expected when the primary sequence of *Pa*Fd is altered to that of *Cp*Fd, but that subtle changes in the orientation of the conserved cysteinyl ligands are likely.

Pseudo-Symmetry of CpFd Reflected in NMR Experiments. The C_2 rotational pseudo-symmetry described above is reflected in the whole range of NMR properties of the cysteinyl proton pairs. These include ^1H and ^{13}C chemical shifts, HH coupling constants (as indicated by the intensities of TOCSY cross-peaks), CH coupling constants, T_1 relaxation, T_2 relaxation (line widths), and cross-peaks in NOESY spectra (Packer et al., 1977; Busse et al., 1991; Bertini et al., 1991, 1992, 1994; Sadek et al., 1993). Data from the present work are summarized in Table 1.[6]

Two similar sets of chemical shifts associated with the eight cysteinyl ligands are observed in the hyperfine-shifted ^1H and ^{13}C NMR spectra of *Cp*Fd. This indicates that clusters I and II have similar, but not equivalent, magnetic environments. The eight lowest field resonances, a−h (a single H^β resonance from each ligand), group as the pairs (a,c), (b,d), (e,f), and (g,h).[6] These pairs can be assigned to the symmetry-related pairs of cysteinyl ligands discussed above. The observation allows classification of the eight sets of hyperfine-shifted ^1H resonances (each containing a H^α and two H^β lines) into four pairs.

Table 1: Summary of NMR Properties of ^1H and ^{13}C Cysteinyl Resonances of Ferredoxin from *Clostridium pasteurianum*

peak[a]	δ-^1H[b] (ppm)	TOCSY[c] geminal[d]	TOCSY[c] vicinal[d]	NOESY[c]	δ-^{13}C (ppm)	HMQC	$^1J_{CH}$[e] (Hz)
a	17.3	s		a′, a″	98.1	w	174
c	15.8	s		c′, c″	96.2	w	184
b	16.2	vw		b′, b″	114.7	w	143
d	14.9	vw		d′, d″, b″	120.2	w	194
f	12.4	m	w	f′	109	m	169
e	13.6	m	w	e′	108.9	m	185
h	11.2	s		h′	92	vw	
g	12.0	s		g′	93.7	vw	
a′	9.3		m	a	98.1	s	196
c′	9.4		m	c	96.2	s	199
b′	5.0			b	114.7	vw	
d′	4.9		vw	d	120.2	vw	
f′	6.2			f	109	vw	
e′	6.8			e	108.9	vw	
h′	8.0		m	h	92	s	184
g′	9.0		m	g	93.7	s	182
a″	9.7			a	83.3	s	188
c″	10.0			c	82	s	202
b″	6.3			b, d	89.5	s	190
d″	7.4			d	92.9	s	190
f″	5.5						
e″	4.5						
h″	3.3						
g″	3.5						

[a] The higher field H^β resonance of each cysteine is labeled a′−h′ corresponding to geminal partner a−h, respectively. Similarly, H^α resonances are labeled a″−h″. [b] Chemical shifts of *Cp*Fd in 50 mM phosphate buffer at pH 7.2 at 298 K referenced to HDO at 4.78 ppm where error is ±0.02 ppm. [c] Recorded with 10 ms mixing time. The pairs of resonances also have similar T_1 and T_2 relaxation times (Bertini et al., 1991; Sadek et al., 1993). [d] Key: s, strong; m, medium; w, weak; vw, very weak cross-peaks. [e] Error in coupling estimated to be ±10 Hz.

NMR of Native CpFd. A fast TOCSY experiment (10 ms mixing time) gives direct intraresidue connectivity and is superior in identifying complete spin systems for each of the eight cysteinyl residues in a single experiment (Sadek et al., 1993). The relative intensities of cross-peaks may be used for stereospecific assignment of cysteinyl β-protons, and this aspect is discussed in more detail below. However, extremely weak geminal and vicinal cross-peaks are associated with the hyperfine-shifted resonances b and d, and a cross-peak between b and b″ (its H^α partner) has not been identified positively. The chemical shift of this missing H^α is easily confirmed in the CH correlation spectrum from an HMQC experiment (Figure 3). Such experiments are now possible at natural abundance for paramagnetic proteins (e.g., *Cau*Fd; Bertini et al., 1994), and the spectra reported here allow detection of six of the C^β and four of the C^α ^{13}C resonances and, for the first time, estimates of one-bond CH

[5] The shortest intercluster distances are between the Fe atoms bound to these residues [Fe58···Fe 67, 8.8 Å (9.6 Å)] and between sulfide ions [S 62···S 69, 9.1 Å (9.3 Å); S 63···S 70, 9.7 Å (10.0 Å)] of the clusters. The first figures correspond to *Pa*Fd crystal structure; figures in parentheses are from the *Cp*Fd structural model. The X-ray structure of *Pa*Fd shows the clusters to be distorted cubes, with a large variation (±2−5°) in bond angles around iron atoms bound to Cys 11, 39 (*Cp*Fd, Cys 11, 40) and Cys 46, 18 (*Cp*Fd, Cys 47, 18), and a small variation (±1−2°) in bond angles around iron atoms bound to Cys 14, 42 (*Cp*Fd, Cys 14, 43) and Cys 8, 36 (*Cp*Fd, Cys 8, 37). The cube side with iron atoms coordinating Cys 14, 46 (cluster I), faces the cube side with iron atoms coordinating Cys 42, 18 (cluster II). The square faces are approximately parallel and twisted by about 20°.

[6] The higher field H^β resonance of each cysteine is labeled a′−h′, corresponding to geminal partner, a−h, respectively. Similarly, H^α resonances are labeled a″−h″.

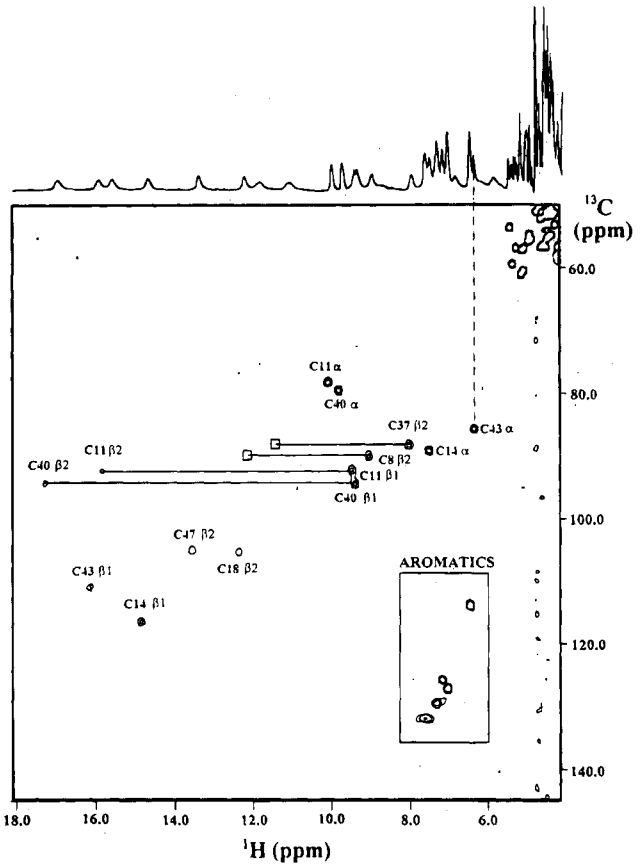

FIGURE 3: HMQC spectrum (500 MHz) of *Cp*Fd showing the CH correlation for hyperfine-shifted resonances of cysteinyl protons and for resonances of aromatic protons. Boxes denote peaks that are observed at lower contour levels.

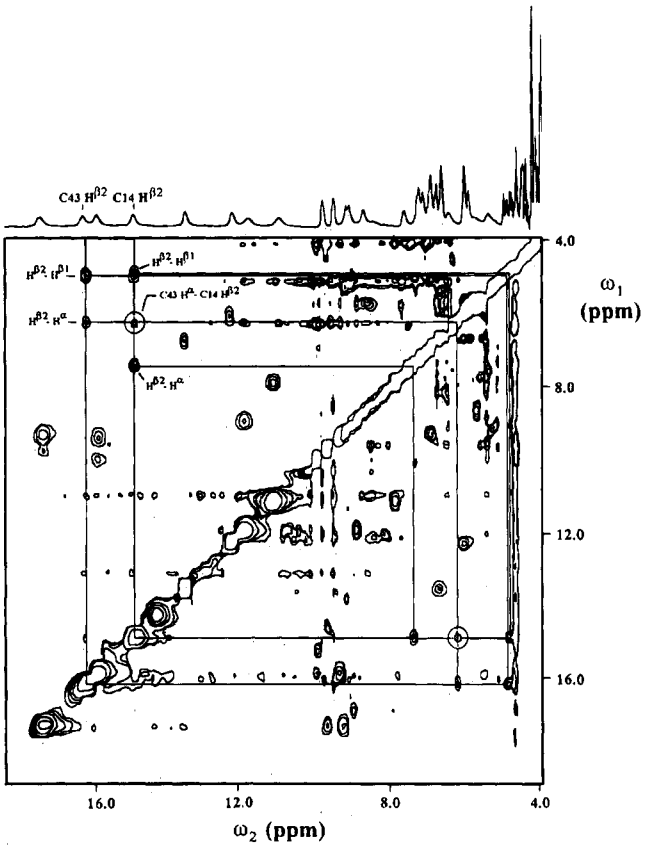

FIGURE 4: NOESY spectrum of *Cp*Fd (10 ms, 500 MHz) showing NOE connectivities between cysteinyl proton resonances.

coupling constants for hyperfine-shifted resonances (Table 1).

The weak geminal coupling implied by weak cross-peaks between resonances b, b′ and d, d′ (Table 1) suggests a special environment for the corresponding cysteinyl residues compared to the others in the molecule. As discussed above, Cys 14 and Cys 43 are the only cysteinyl residues whose side chains are located directly between the clusters, and the *Cp*Fd model (see Figure 2) suggests Cys 43 H^{α}–Cys 14 H^{β} distances of less than 3 Å, the effective detection limit in the vicinity of these paramagnetic clusters (Sette et al., 1993). The observation of an NOE cross-peak between d and b″ in NOESY spectra acquired with mixing times of 5–10 ms [Figure 4; see also Busse et al. (1991)] allows sequence-specific assignment of these resonances as d:Cys 14 H^{β}, and b″:Cys 43 H^{α}. The equivalent NOE cross-peak was used for initial assignment in *Cau*Fd by Bertini et al. (1994). However, it is difficult to use this NOE cross-peak for a stereospecific assignment. Both the X-ray structure of *Pa*Fd (Backes et al., 1991) and the *Cp*Fd model indicate that NOE cross-peaks due to both Cys 43 (42) H^{α}–Cys 14 $H^{\beta 1}$ and Cys 43 (42) H^{α}–Cys 14 $H^{\beta 2}$ may be present. The assignment of residues Cys 14, 43 is discussed in more detail below.

Design and Characterization of Mutant Proteins. Mutant forms of *Cp*Fd were used to facilitate further sequence-specific assignments. As hyperfine-shifted resonances are very sensitive to amino acid substitution, G12A and G41A mutants were designed to produce a stable product with minor local structural changes (hence small chemical shift perturbations) in cluster I (Cys 8, 11, 14, 47) by changing Gly 12 to Ala or in cluster II (Cys 37, 40, 43, 18) by changing the symmetry-related Gly 41 to Ala (Figure 1). The structural model for *Cp*Fd indicates that both Gly 12 and Gly 41 side chains are located on the surface of the protein, and hence, mutation to Ala would produce minimal structural perturbation. However, they form part of the characteristic CysXXCysGlyXCysAla sequences, and so individual cysteinyl ligands are directly adjacent to the site of mutation (Cys 11, 40) or within two (Cys 14, 43) or four (Cys 8, 37) residues (Figure 1). The *Pa*Fd crystal structure indicates that the peptide NH functions of both Gly 12 and 40(41) are involved in NH···S hydrogen bonding either directly to the cluster sulfides (Gly 12 NH···S60, Gly 40(41) NH···S71)[3] or to the adjacent cysteinyl ligands (Gly 12 NH···Cys 11 S^{γ}, Gly 40(41) NH···Cys 39(40) S^{γ}.[7] The equivalent interactions are maintained in the *Cp*Fd model. In addition, H^{α} protons from both Gly 12 and 41 are in van der Waals contact with the aromatic rings of Phe 30 and Tyr 2, respectively. These interactions will be influenced by the changes in structural and electronic effects within the mutated residues. Consequently, the double mutant G12,41A was included to monitor localization of structural changes in the single mutants.

A *Cp*Fd gene fragment was isolated via the polymerase chain reaction using genomic DNA and primers based upon the reported gene sequence (Graves et al., 1985). The mutant proteins were isolated as described in the Materials and Methods section. Sequencing of the first 15 residues of the recombinant and G12A proteins confirmed their identity.

[7] Although not discussed specifically (Backes et al., 1991), the atomic coordinates of *Pa*Fd suggest that these NH···S bonds are possible.

Table 2: Sequential Assignment and ^{1}H Chemical Shift Changes (ppm) for Lowest Field Cysteinyl H$^\beta$ Resonances upon Mutation in Oxidized *Cp*Fd

peak	assignment[b]	cluster	native[a]	ΔG12A[c]	ΔG41A[c]	predicted ΔG12,41A[d]	ΔG12,41A[c]
a	*Cys 40 H$^{\beta 2}$	II	17.26	−0.05	+0.17	+0.12	+0.13
b	Cys 43 H$^{\beta 1}$	II	16.16	+0.04	+0.14	+0.18	+0.14
c	*Cys 11 H$^{\beta 2}$	I	15.82	+0.38	−0.04	+0.34	+0.38
d	Cys 14 H$^{\beta 1}$	I	14.89	+0.12	0.00	+0.12	+0.14
e	*Cys 47 H$^{\beta 2}$	I	13.55	+0.11	+0.07	+0.18	+0.16
f	*Cys 18 H$^{\beta 2}$	II	12.36	0.00	−0.05	−0.05	−0.06
g	*Cys 8 H$^{\beta 1}$	I	11.97	−0.09	+0.03	−0.06	−0.08
h	*Cys 37 H$^{\beta 1}$	II	11.19	0.00	+0.02	+0.02	+0.01

[a] Chemical shifts of *Cp*Fd in 50 mM phosphate buffer at pH 7.2 at 298 K referenced to HDO at 4.78 ppm. Error ±0.02 ppm. [b] The stereospecific assignment shown is that published by Bertini et al. (1994). The asterisk (*) designates cysteines that can be stereospecifically assigned from our data. [c] Measured as the difference in chemical shift between the native and the mutated proteins. Positive shifts are downfield from native *Cp*Fd. [d] The addition of ΔG12A and ΔG41A in ppm.

As observed previously (Baur et al., 1990; Smith et al., 1991; Davasse & Moulis, 1992), characteristic properties of native and recombinant *Cp*Fd were indistinguishable (specific activity, 5.2 ± 0.3 units; 7.5 ± 0.1 Fe atoms/molecule; A_{390}/A_{280}, 0.81; $E_{1/2}$, −391 ± 5 mV vs standard hydrogen electrode). NOESY spectra were also virtually identical, a very sensitive test of identity. The G12A and G41A mutants showed very similar properties: specific activities seem to be marginally lower (4.3 and 4.7 units, respectively) than the native form under the conditions of the assay. Properties of the double mutant G12,41A varied significantly (specific activity, 2.8 units; $E_{1/2}$, −406 mV). It is less stable in air in dilute solution but stable at the higher concentrations and anaerobic conditions of the NMR measurements. The NMR experiments indicate that the overall structure of the clusters and folding of the polypeptide chains have been conserved in these mutants.

Comparison of NMR Properties of Native and Mutant CpFd. The chemical shifts observed for resonances a−h in the native protein together with the shift changes induced by mutations G12A, G41A, and G12,41A are listed in Table 2. The corresponding 1D ^{1}H NMR spectra are shown in Figure 5.

The shift changes range from 0 to 0.38 ppm. As discussed above, the cysteinyl residues that are closest to the site of mutation are expected to show the largest shift change. The assumption of minor highly localized structural changes is strongly supported by the observed additivity of the chemical shift changes, i.e., the sum of corresponding chemical shift changes for a given resonance in the single mutants, ΔG12A + ΔG41A, is equal to the corresponding chemical shift change seen in the double mutant, ΔG12,41A (Table 2).

The resonances a and b can be associated immediately with cluster II (G41A), and c and d can be associated with cluster I (G12A), consistent with the above assignment of b″ (Cys 43 H$^\alpha$) and d (Cys 14 H$^\beta$). Given the local nature of the perturbation, the effect on more distant cysteines is expected to be smaller and comparable to the secondary effects arising from the conformational changes of other amino acid residues close to the sites of mutation. Consequently, cluster-specific assignment of resonances e−h is not so straightforward; in particular, resonance e shows a significant shift in both mutant proteins while h is unshifted in both. Nevertheless, an assignment of g to cluster I and f to cluster II follows from the relative magnitudes of the observed shifts in the mutant and native proteins. The pairings (e,f) and (g,h) complete a cluster-specific assignment (Table 2) which is the same as that deduced on the basis of differential shifts upon reduction (Bertini et al., 1992). Sequence-specific assignments were aided by 2D experiments on all three mutants, and the relevant features are discussed below.

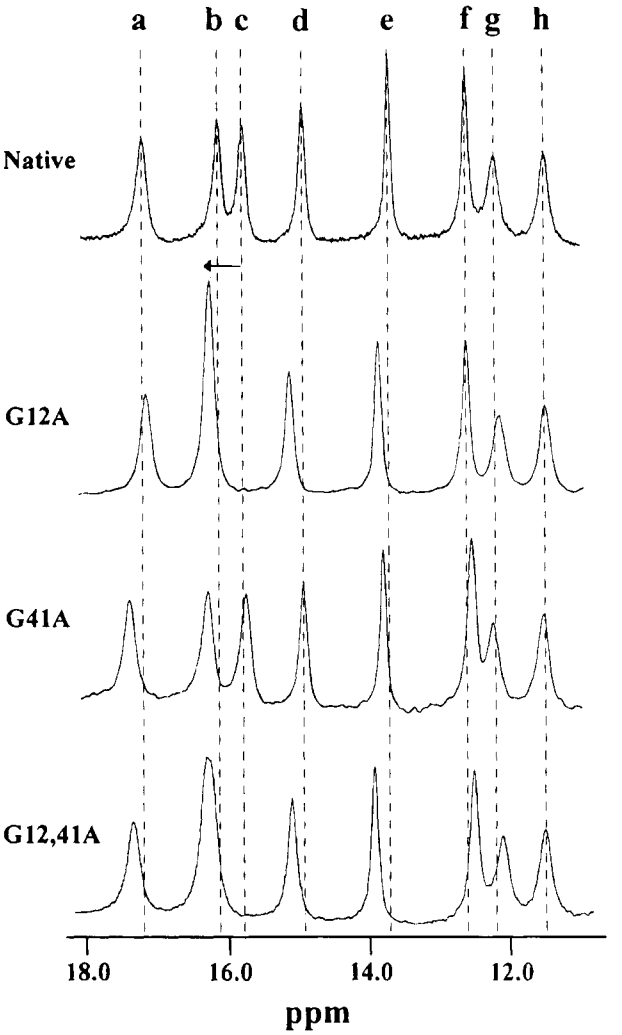

FIGURE 5: Hyperfine-shifted resonances of native ferredoxin and the G12A, G41A, and G12,41A mutant forms. The arrow indicates the shift to lower field for resonance c in the G12A mutant.

Assignment of Cys 11 and Cys 40. By far, the largest change in chemical shifts listed in Table 2 is exhibited by resonance c in the G12A mutant, allowing its assignment to Cys 11, adjacent to the site of mutation. Resonances a and b show the greatest chemical shift changes in the G41A mutant. Resonance b has already been assigned to Cys 43

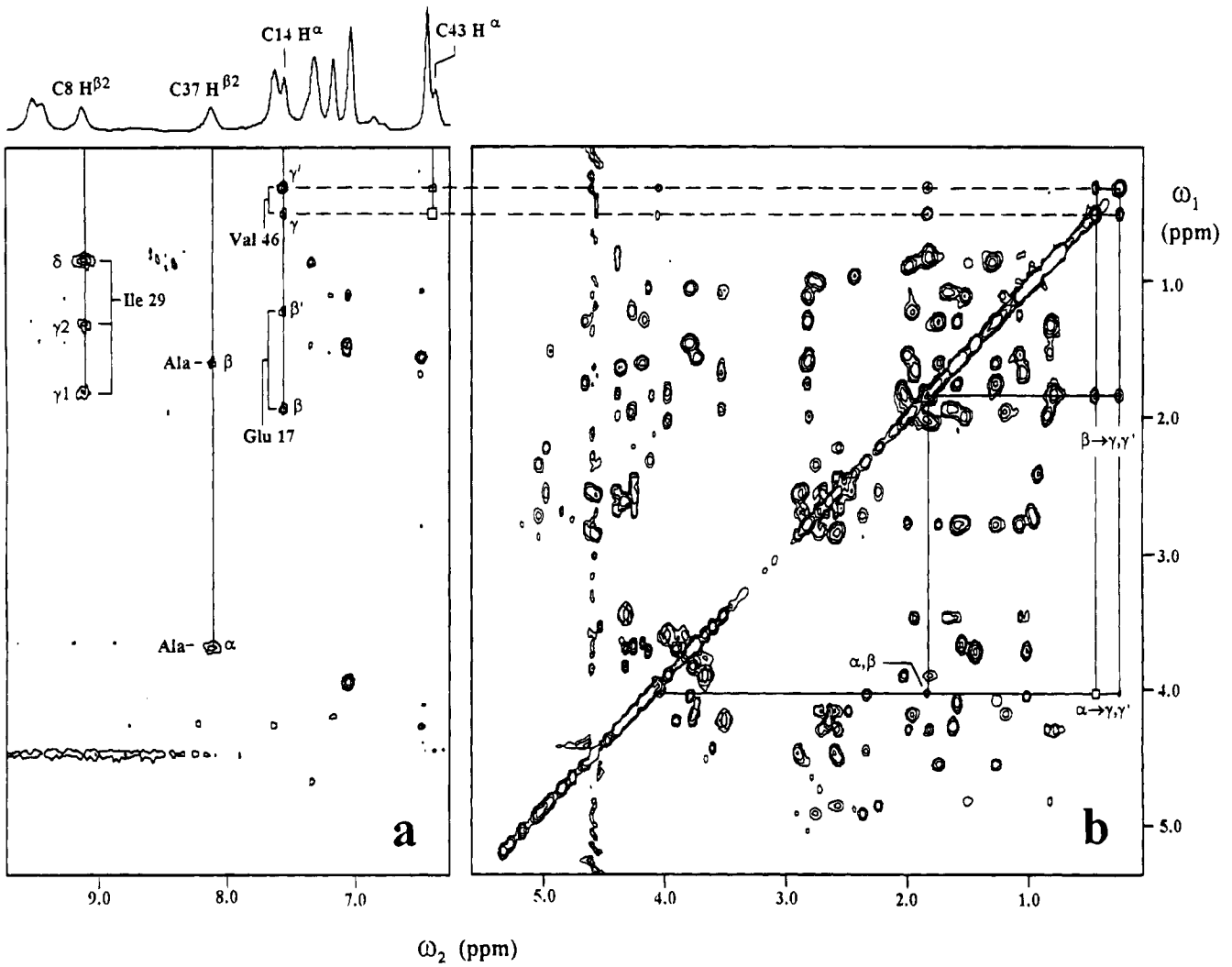

FIGURE 6: (a) NOESY spectrum of *Cp*Fd (50 ms, 500 MHz) showing the long-range NOE connectivities with cysteinyl protons. (b) TOCSY spectrum (40 ms, 400 MHz) identifying the Val 46 spin system. Boxes denote peaks observed at lower levels.

H^{β}, allowing assignment of a to Cys 40, related to Cys 11 by the C_2 pseudo-axis. NOE interactions involving Cys 11 and Cys 40 have not been identified positively:[8] the structural model indicates that the only H···H separation of less than 3 Å involving a Cys 11 or a Cys 40 β-proton is that between Cys 11 and Val 9 $(CH_3)^{\gamma}$.

Assignment of Cys 14 and Cys 43. The assignment of resonances b and d to Cys 43 H^{β} and Cys 14 H^{β} was based on the NOE data for native *Cp*Fd discussed above. The assignment is supported by the largest or second largest shift changes being observed for resonance b in G41A and resonance d in G12A: Cys 43 and Cys 14 are separated by a single residue from the point of mutation.

The assignments are supported further by the observation of NOE interactions between H^{α} of these residues (resonances b″ and d″) and of non-cysteinyl protons detected in a 50-ms NOESY experiment. As shown in Figure 6, four strong NOE connectivities exist between resonance d″ (Cys 14 H^{α}) and resonances at 0.36, 0.58, 1.31, and 2.06 ppm, and two exist between resonance b″ (Cys 43 H^{α}) and resonances at 0.36 and 0.58 ppm. TOCSY and NOESY experiments at two different temperatures (298 and 303 K) confirmed that these cross-peaks originate from b″ and not from f′ (Table 1). TOCSY spectra identify the resonances at 0.36 and 0.58 ppm as valine methyl protons by their characteristic spin pattern. This spin system is assigned specifically to Val 46 through sequential $NH_i-H^{\alpha}_{i+1}$, $NH_i-H^{\beta}_{i+1}$, and NH_i-NH_{i+1} connectivities with Asn 45, confirmed recently in both *Cp*Fd and *Cau*Fd (Gaillard et al., 1993a; S. D. B. Scrofani, R. T. C. Brownlee, M. Sadek, and A. G. Wedd, manuscript in preparation). The equivalent resonances in *Cau*Fd were misassigned originally to Ile 23 (Bertini et al., 1994). The primary sequence of *Cp*Fd (Figure 1) shows that Val 46 occurs in the pentapeptide segment (residues 43−47) linking the clusters, and the *Cp*Fd model suggests that the methyl groups of Val 46 are situated in close proximity (<4 Å) to the H^{α} protons of both Cys 14 and Cys 43. It is the only valine residue that can have such detectable NOE interactions.

NOE cross-peaks also exist between d″ (Cys 14 H^{α}) and resonances at 1.31 and 2.06 ppm. The latter have been identified as H^{β} resonances of a single spin system, assigned

[8] NOESY spectra (10 ms mixing time) detect long-range NOE interactions between resonances a, b, c, e, g, and h and unidentified methyl groups of valine and/or isoleucine residues. However, low resolution (partially due to the enhancement of broad peaks via processing) and considerable overlap in the methyl resonance region prevented unambiguous identification of these resonances. Resonance d shows an NOE cross-peak with a high field resonance, attributed to the methyl group of Val 46.

to Glu 17 via the observation of NOE NH_i-NH_{i+1} interactions with Ser 16. In addition, NOE connectivities between its H^{β} resonances and the methyl groups of Val 46 are observed (S. D. B. Scrofani, R. T. C. Brownlee, M. Sadek, and A. G. Wedd, manuscript in preparation).

Assignment of Cys 8 and Cys 37. Resonances g and h have been assigned to clusters I and II, respectively (Table 2). The sequential assignment of these resonances is derived from NOESY experiments on native *Cp*Fd and from the *Cp*Fd structural model. Assignment of g′ to the Cys 8 spin system is supported by NOE connectivities with the $(CH_3)^{\delta}$, $(CH_2)^{\gamma}$, and $(CH_3)^{\gamma}$ resonances of an isoleucine residue (Figure 6). The structural model indicates that H^{β} and $(CH_3)^{\gamma}$ hydrogens of Ile 29 are within 3 Å of Cys 8 $H^{\beta 2}$ and that Ile 29 is a surface residue, with its side chain free to rotate unhindered by other residues in the region. Such rotation about both the $C^{\alpha}-C^{\beta}$ and $C^{\beta}-C^{\gamma}$ bonds of Ile 29 rationalizes the observation of these NOE interactions, since Cys 8 is constrained with its β2-proton pointing directly toward Ile 29. A similar NOE connectivity has been observed (Bertini et al., 1994) between the equivalent Cys 8 $H^{\beta 2}$ hydrogen in *Cau*Fd and the unique Arg 29 in that protein: residue 29 is an isoleucine in *Cp*Fd (the corresponding residue in *Pa*Fd is Ile 28). These observed NOE interactions provide unambiguous stereospecific assignment for these cysteinyl β-protons, in agreement with TOCSY experiments described below.

Cys 8 and Cys 37 are related by the C_2 pseudo-axis of symmetry, implying assignment of h to Cys 37. Resonance h shows NOE connectivities (5−50 ms NOESY) with resonances at 3.90 and 1.70 ppm (Figure 6). A phase-sensitive DQ-COSY experiment, which readily identifies AX_3 spin systems (Dalvit et al., 1986), indicates that these resonances belong to H^{α} and $(CH_3)^{\beta}$ groups of separate alanine residues (S. D. B. Scrofani, R. T. C. Brownlee, M. Sadek, and A. G. Wedd, manuscript in preparation). The *Cp*Fd structural model suggests but cannot confirm that Ala 1 and Ala 34 are the residues involved.

Assignment of Cys 47 and Cys 18. The remaining pair of resonances (e, f) must be assigned to Cys 47, Cys 18 in agreement with the previous assignment (Bertini et al., 1994). While the structural model of *Cp*Fd indicates some HH distances of around 3 Å involving Cys 47, Cys 18 β-protons, no identifiable[8] NOE interactions have been detected.

Other Mutants of CpFd. Gaillard and co-workers (1993b) have prepared a series of *Cp*Fd mutant proteins, two of which substituted lysine residues for the highly conserved prolines at positions 19 and 48, adjacent to Cys 18 and Cys 47. The oxidized form of these P19K and P48K mutants exhibit dramatic changes in chemical shifts for some resonances (range: −2.3 to +1.5 ppm), making assignment difficult. An assignment consistent with the present work follows if, as predicted by the *Cp*Fd structural model, the extended lysine side chain, $(CH_2)_4NH_3^+$, positions its ammonium ion head group close to Cys 40 and Cys 11 in mutants P19K and P48K, respectively. The charge and hydrogen-bonding capability of lysine indicate that the most shifted resonances a and c should arise from Cys 40 and Cys 11, respectively. Further assignments of Cys 47 (e) and Cys 18 (f) follow on the basis of their proximity to the sites of mutation. The dramatic effects of structural change upon hyperfine-shifted resonances is highlighted in these proline to lysine mutants.

Stereospecific Assignment. Such assignments are difficult to achieve for paramagnetic proteins where the effects of magnetic anisotropy complicate both theory and experiment (La Mar & de Ropp, 1993). A stereospecific assignment of cysteinyl β-protons for *Cau*Fd and, by extension, for *Cp*Fd has been made assuming the X-ray structure of *Pa*Fd (Bertini et al., 1994). The modeling aspect of the present work suggests that the orientation of the cysteinyl residues is sensitive to primary structure. We are, however, able to provide experimental support for a number of the assignments (marked with asterisks in Table 2).

Stereospecific assignment may be achieved from experimental NMR and X-ray structural data by various approaches such as theoretical estimation of the hyperfine shifts, relaxation properties of hyperfine-shifted resonances, vicinal HH coupling rationalized by the Karplus relationship, or NOE interactions between the β-protons and protons of other residues. Although a full set of NMR data is not available for all 16 cysteinyl β-protons of *Cp*Fd and related proteins, TOCSY experiments provide more information.

The intensities of cross-peaks in TOCSY spectra are related to the magnitude of coupling between the corresponding protons. Although the relationship is not simple (Remerowski et al., 1989), the oscillatory behavior of intensities can be neglected for short mixing times. The intensities of cross-peaks between the resonances corresponding to the vicinal cysteinyl protons may provide the direct experimental evidence necessary for a stereospecific assignment of cysteinyl β-protons. The standard Karplus relationship for vicinal coupling may not apply in the present case due to paramagnetic effects. However, application to the present case and a consideration of vicinal dihedral angles provide a prediction of the relative intensities of TOCSY cross-peaks. In particular, relatively strong $H^{\beta 1}-H^{\alpha}$ cross-peaks for Cys 40, 11 and $H^{\beta 2}-H^{\alpha}$ cross-peaks for Cys 37, 8 and Cys 18, 47 are anticipated. The rest should be weak or not present. Strong TOCSY cross peaks are indeed observed for vicinal coupling of protons associated with the resonances (a′, c′), (h′, g′), and (f, e). The data allow a tentative stereospecific assignment for 12 out of the 16 cysteinyl β-protons (Cys 40, 11, 18, 47, 37, 8) of *Cp*Fd. This assignment is consistent with the previous assignment of *Cau*Fd (Bertini et al., 1994).

CONCLUSIONS

This work reports a complete sequence-specific assignment of cysteinyl ligand resonances in *Cp*Fd derived from 2D NMR data on native *Cp*Fd and a range of specifically designed mutants. It complements the assignment derived for *Cau*Fd and applied to *Cp*Fd by analogy (Bertini et al., 1994). In particular, the convincing identification of the Cys, 11, 40 and Cys 8, 37 pairs in the present work strengthens confidence in the sequence-specific assignments and in the mechanism of spin delocalization deduced from that assignment.

The chemical shifts of the hyperfine-shifted resonances of interest to the present work are extremely sensitive to structural change. Such effects were minimized for assignment purposes by taking advantage of the pseudo 2-fold symmetry of *Cp*Fd to design complementary single and double mutants which produced minimal local structural

changes. Observed chemical shifts could then be related to specific cysteinyl residues.

ACKNOWLEDGMENT

R.T.C.B. and A.G.W. thank the Australian Research Council for financial support. S.D.B.S., G.A.V., and P.S.B. would like to acknowledge the receipt of an Australian Postgraduate Research Scholarship. Dr. R. Norton (Biomolecular Research Institute, Melbourne) is thanked for generous access to a Bruker AMX-500 spectrometer.

REFERENCES

Adman, E. T., Sieker, L. C., & Jensen, L. H. (1973) *J. Biol. Chem. 248*, 3987−3996.
Armstrong, F. A., Hill, H. A. O., Oliver, B. N., & Walton, N. J. (1984) *J. Am. Chem. Soc. 106*, 921−923.
Backes, G., Mino, Y., Loehr, T. M., Meyer, T. E., Cusanovich, M. A., Sweeney, W. V., Adman, E. T., & Sanders-Loehr, J. (1991) *J. Am. Chem. Soc. 113*, 2055−2064.
Banci, L., Bertini, I., Carloni, P., Luchinat, C., & Orioli, P. L. (1992) *J. Am. Chem. Soc. 114*, 10683−10689.
Banci, L., Bertini, I., Capozzi, F., Carloni, P., Ciurli, S., Luchinat, C., & Piccioli, M. (1993) *J. Am. Chem. Soc. 115*, 3431−3440.
Baur, J. R., Graves, M. C., Feinberg, B. A., & Ragsdale, S. W. (1990) *Biofactors 2*, 197−203.
Bax, A., & Davis, D. G. (1985) *J. Magn. Reson. 65*, 355−360.
Bax, A., Griffey, R. H., & Hawkins, B. L. (1980) *J. Am. Chem. Soc. 102*, 4849−4851.
Bax, A., Griffey, R. H., & Hawkins, B. L. (1983) *J. Magn. Reson. 55*, 301−315.
Bertini, I., & Luchinat, C. (1986) *NMR of Paramagnetic Molecules in Biological Systems*, Benjamin/Cummings Publishing Co., Menlo Park, CA.
Bertini, I., Briganti, F., Luchinat, C., & Scozzafava, A. (1990) *Inorg. Chem. 29*, 1874−1880.
Bertini, I., Briganti, F., Luchinat, C., Messori, L., Monnanni, R., Scozzafava, A., & Vallini, G. (1991) *FEBS Lett. 289*, 253−256.
Bertini, I., Briganti, F., Luchinat, C., Messori, L., Monnanni, R., Scozzafava, A., & Vallini, G. (1992) *Eur. J. Biochem. 204*, 831−839.
Bertini, I., Turano, P., & Vila, A. J. (1993) *Chem. Rev. 93*, 2833−2932.
Bertini, I., Capozzi, F., Luchinat, C., Piccioli, M., & Vila, A. J. (1984) *J. Am. Chem. Soc. 116*, 651−660.
Blundell, T., Sibanda, B. L., & Pearl, L. (1983) *Nature 304*, 273−275.
Blundell, T., Carney, D., Gardner, S., Hayes, F., Howlin, B., Hubbard, T., Overington, J., Singh, D. A., Sibanda, B. L., & Sutcliffe, M. (1988) *Eur. J. Biochem. 172*, 513−520.
Braunschweiler, L., & Ernst, R. R. (1983) *Mol. Phys. 48*, 535−560.
Bruschi, M., & Guerlesquin, F. (1988) *FEMS Microbiol. Rev. 54*, 155−176.
Busse, S. C., La Mar, G. N., & Howard, J. B. (1991) *J. Biol. Chem. 266*, 23714−23723.
Cammack, R. (1992) *Adv. Inorg. Chem. 38*, 281−313.
Chae, Y. K., Abildgaard, F., Mooberry, E. S., & Markley, J. L. (1994) *Biochemistry 33*, 3287−3295.
Cheng, H., Grohmann, K., & Sweeney, W. (1992) *J. Biol. Chem. 267*, 8073−8080.
Coghlan, V. M., & Vickery, L. E. (1991) *J. Biol. Chem. 266*, 18606−18612.
Dalvit, C., Rance, M., & Wright, P. E. (1986) *J. Magn. Reson. 69*, 1986, 356−361.
Davasse, V., & Moulis, J.-M. (1992) *Biochem. Biophys. Res. Commun. 185*, 341−349.
Freeman, R., Kempsell, S. P., & Levitt, M. (1980) *J. Magn. Reson. 38*, 453−479.
Gaillard, J., Moulis, J.-M., & Meyer, J. (1987) *Inorg. Chem. 26*, 320−324.
Gaillard, J., Albrand, J.-P., Moulis, J.-M., & Wemmer, D. E. (1992) *Biochemistry 31*, 5632−5639.
Gaillard, J., Moulis, J.-M., Kümmerle, R., & Meyer, J. (1993a) *Magn. Reson. Chem. 31*, S27−S33.
Gaillard, J., Quinkal, I., & Moulis, J.-M. (1993b) *Biochemistry 32*, 9881−9887.
George, D. G., Hunt, L. T., Yeh, L.-S., & Barker, W. C. (1985) *J. Mol. Evol. 22*, 20−31.
Graves, M. C., Mullenbach, G. T., & Rabinowitz, J. C. (1985) *Proc. Natl. Acad. Sci. U.S.A. 82*, 1653−1657.
Gross, K.-H., & Kalbitzer, H. R. (1988) *J. Magn. Reson. 76*, 87−99.
Kunkel, T. A. (1985) *Proc. Natl. Acad. Sci. U.S.A. 82*, 488−492.
La Mar, G. N., & de Ropp, J. S. (1993) in *Biological Magnetic Resonance. Vol. 12, NMR of Paramagnetic Molecules* (Berliner, L. J., & Reuben, J., Eds.) Plenum Press, New York.
Langen, R., Jensen, G. M., Jacob, U., Stephens, P. J., & Warshel, A. (1992) *J. Biol. Chem. 267*, 25625−25627.
Macura, S., & Ernst, R. R. (1980) *Mol. Phys. 41*, 95−117.
Marion, D., & Wüthrich, K. (1983) *Biochem. Biophys. Res. Commun. 113*, 967−974.
Mortenson, L. E., Valentine, R. C., & Carnahan, J. E. (1962) *Biochem. Biophys. Res. Commun. 7*, 448−452.
Moulis, J.-M., & Meyer, J. (1982) *Biochemistry 21*, 4762−4771.
Oh, B.-H., & Markley, J. L. (1990a) *Biochemistry 29*, 3993−4004.
Oh, B.-H., & Markley, J. L. (1990b) *Biochemistry 29*, 4004−4011.
Oh, B.-H., & Markley, J. L. (1990c) *Biochemistry 29*, 4012−4017.
Packer, E. L., Sweeney, W. V., Rabinowitz, J. C., Sternlicht, H., & Shaw, E. N. (1977) *J. Biol. Chem. 252*, 2245−2253.
Palmer, G. (1991) *Struct. Bonding (Berlin) 75*.
Rabinowitz, J. C. (1972) *Methods Enzymol. 24*, 431−446.
Remerowski, M. L., Glaser, S. J., & Drobny, G. P. (1989) *Mol. Phys. 68*, 1191−1218.
Sadek, M., Brownlee, R. T. C., Scrofani, S. D. B., & Wedd, A. G. (1993) *J. Magn. Reson. Ser. B 101*, 309−314.
Saiki, R. K., Gelfand, D. H., Stoffel, S., Scharf, S. J., Higuchi, R., Horn, G. T., Mullis, K. B., & Erlich, H. A. (1988) *Science 239*, 487−491.
Sambrook, J., Fritsch, E. F., & Maniatis, T. (1989) *Molecular Cloning: A Laboratory Manual*, 2nd ed., Vols. 1−3, Cold Spring Harbor Laboratory Press, Cold Spring Harbor, NY.
Sette, M., de Ropp, J. S., Hernandez, G., & La Mar, G. N. (1993) *J. Am. Chem. Soc. 115*, 5237−5245.
Shaka, A. J., Barker, P. B., & Freeman, R. (1985) *J. Magn. Reson. 64*, 547−552.
Smith, E. T., Feinberg, B. A., Richards, J. H., & Tomich, J. M. (1991) *J. Am. Chem. Soc. 113*, 688−689.
States, D. J., Haberkorn, R. A., & Ruben, D. J. (1982) *J. Magn. Reson. 48*, 286−298.
Studier, F. W. (1991) *J. Mol. Biol. 219*, 37−44.
Thauer, R. K., & Schönheit, P. (1982) in *Iron-Sulfur Proteins* (Spiro, T., Ed.) p 329, Academic Press, New York.
Zanetti, G., & Curti, B. (1980) *Methods Enzymol. 69*, 250−255.